FDCs express clusterin (current study and reference [12]), and its expression appears to be up-regulated during TSE disease, it is plausible that clusterin is likewise released by FDCs as an activating factor for themselves and/or neighbouring germinal centre B cells [12], which might accelerate abnormal PrP accumulation.

In the Peyer's patches and appendices, some lymphoid follicles showed no detectable PrP deposition, but revealed enhanced clusterin immunoreactivity. Although it is possible that small amounts of undetectable abnormal PrP molecules were present in these follicles, enhanced clusterin expression at this site was probably due to non-specific immune stimulation. Clusterin-enhanced lymphoid follicles were confirmed even in the Peyer's patches of non-infected control mice and in the appendices of non-CJD control cases. The continual exposure of the intestinal lymphoreticular system to a variety of antigens or stress conditions might account for the enhanced clusterin expression in non-TSE affected subjects in comparison with the spleens. The reasons why the regulation of clusterin expression on FDCs in the intestine and other lymphoid tissues appears to differ in uninfected hosts are unknown and therefore worthy of further investigation.

We employed a detergent autoclaving method for PrP detection in this study and found that this method significantly improved sensitivity, especially when analysing the lymphoreticular pathology of TSEs. The early detection of PrP accumulation on FDCs might aid the detection of scrapie transmissibility, and the diagnosis of human variant CJD, for example on tonsil biopsy specimens. Detergent autoclaving also provides a less harsh pretreatment for antigen retrieval, avoids tissue damage, and reduces non-specific background staining. Prolonged formalin fixation of tissue samples results in a considerable reduction of PrP immunoreactivity. This effect might be overcome by modifying the concentration of detergents and/or autoclaving time without causing significant tissue damage.

In conclusion, we have demonstrated that clusterin expression was increased in association with abnormal PrP deposits not only in the CNS [13] but also in the peripheral lymphoreticular system. The observed co-localization and correlative expression of these proteins implies that clusterin might have an important role in PrP pathogenesis in the TSEs, perhaps as a chaperone-like molecule. In keeping with this suggestion, Kempster and associates reported that clusterin-deficient mice inoculated i.p. with mouse-passaged BSE agent had an increased incubation time in comparison with wild-type mice [31]. Thus clusterin might influence the accumulation and/or aggregation of PrP on FDCs, and affect disease progression. Comparative transmission studies using clusterin-deficient mice inoculated with a variety of TSE agent strains by various peripheral routes of exposure will provide further insights into the role of clusterin in TSE pathogenesis.

Acknowledgements

This work was supported by grants to K Doh-ura and T Iwaki from the Ministry of Health, Labour and Welfare, Japan and a grant to K Sasaki from the Japan Society for the Promotion of Science. We thank Ms K Hatanaka, Ms S Nagae, and Mr S Mawatari for their excellent technical assistance. Part of this study was carried out at the Morphology Core, Graduate School of Medical Sciences, Kyushu University. LTβR-Ig and Hu-Ig were kindly provided by Dr Jeffrey Browning (Biogen Inc, Cambridge, MA, USA) and requests for these reagents should be addressed to Jeff_Browning@biogen.com.

References

1. Collinge J, Sidle KC, Meads J, Ironside J, Hill AF. Molecular analysis of prion strain variation and the aetiology of 'new variant' CJD. *Nature* 1996;**383:**685–690.
2. Bruce ME, Will RG, Ironside JW, McConnell I, Drummond D, Suttie A, *et al.* Transmissions to mice indicate that 'new variant' CJD is caused by the BSE agent. *Nature* 1997;**389:**498–501.
3. Hill AF, Desbruslais M, Joiner S, Sidle KC, Gowland I, Collinge J, *et al.* The same prion strain causes vCJD and BSE. *Nature* 1997;**389:**448–450, 526 .
4. Hill AF, Zeidler M, Ironside J, Collinge J. Diagnosis of new variant Creutzfeldt-Jakob disease by tonsil biopsy. *Lancet* 1997;**349:**99–100.
5. Kitamoto T, Muramoto T, Mohri S, Doh-Ura K, Tateishi J. Abnormal isoform of prion protein accumulates in follicular dendritic cells in mice with Creutzfeldt-Jakob disease. *J Virol* 1991;**65:**6292–6295.
6. van Keulen LJ, Schreuder BE, Meloen RH, Mooij-Harkes G, Vromans ME, Langeveld JP. Immunohistochemical detection of prion protein in lymphoid tissues of sheep with natural scrapie. *J Clin Microbiol* 1996;**34:**1228–1231.
7. Jeffrey M, McGovern G, Goodsir CM, Brown KL, Bruce ME. Sites of prion protein accumulation in scrapie-infected mouse spleen revealed by immuno-electron microscopy. *J Pathol* 2000;**191:**323–332.
8. Race R, Oldstone M, Chesebro B. Entry versus blockade of brain infection following oral or intraperitoneal scrapie administration: role of prion protein expression in peripheral nerves and spleen. *J Virol* 2000;**74:**828–833.
9. Glatzel M, Heppner FL, Albers KM, Aguzzi A. Sympathetic innervation of lymphoreticular organs is rate limiting for prion neuroinvasion. *Neuron* 2001;**31:**25–34.
10. Tschopp J, Chonn A, Hertig S, French LE. Clusterin, the human apolipoprotein and complement inhibitor, binds to complement C7, C8-beta, and the b domain of C9. *J Immunol* 1993;**151:**2159–2165.
11. French LE, Wohlwend A, Sappino AP, Tschopp J, Schifferli JA. Human clusterin gene expression is confined to surviving cells during in vitro programmed cell death. *J Clin Invest* 1994;**93:**877–884.
12. Huber C, Thielen C, Seeger H, Schwarz P, Montrasio F, Wilson MR, *et al.* Lymphotoxin-beta receptor-dependent genes in lymph node and follicular dendritic cell transcriptomes. *J Immunol* 2005;**174:**5526–5536.
13. Sasaki K, Doh-ura K, Ironside JW, Iwaki T. Increased clusterin (apolipoprotein J) expression in human and mouse brains infected with transmissible spongiform encephalopathies. *Acta Neuropathol (Berl)* 2002;**103:**199–208.
14. Wilson MR, Easterbrook-Smith SB. Clusterin is a secreted mammalian chaperone. *Trends Biochem Sci* 2000;**25:**95–98.
15. Sasaki K, Doh-ura K, Wakisaka Y, Iwaki T. Clusterin/apolipoprotein J is associated with cortical Lewy bodies: immunohistochemical study in cases with alpha-synucleinopathies. *Acta Neuropathol (Berl)* 2002;**104:**225–230.
16. Chiesa R, Angeretti N, Lucca E, Salmona M, Tagliavini F, Bugiani O, *et al.* Clusterin (SGP-2) induction in rat astroglial

cells exposed to prion protein fragment 106–126. *Eur J Neurosci* 1996;**8:**589–597.
17. McHattie S, Edington N. Clusterin prevents aggregation of neuropeptide 106–126 in vitro. *Biochem Biophys Res Commun* 1999;**259:**336–340.
18. Fischer M, Rulicke T, Raeber A, Sailer A, Moser M, Oesch B, *et al.* Prion protein (PrP) with amino-proximal deletions restoring susceptibility of PrP knockout mice to scrapie. *EMBO J* 1996;**15:**1255–1264.
19. Thackray AM, Klein MA, Bujdoso R. Subclinical prion disease induced by oral inoculation. *J Virol* 2003;**77:**7991–7998.
20. Race RE, Priola SA, Bessen RA, Ernst D, Dockter J, Rall GF, *et al.* Neuron-specific expression of a hamster prion protein minigene in transgenic mice induces susceptibility to hamster scrapie agent. *Neuron* 1995;**15:**1183–1191.
21. Mabbott NA, Mackay F, Minns F, Bruce ME. Temporary inactivation of follicular dendritic cells delays neuroinvasion of scrapie. *Nat Med* 2000;**6:**719–720.
22. Mabbott NA, Young J, McConnell I, Bruce ME. Follicular dendritic cell dedifferentiation by treatment with an inhibitor of the lymphotoxin pathway dramatically reduces scrapie susceptibility. *J Virol* 2003;**77:**6845–6854.
23. Mabbott NA, Williams A, Farquhar CF, Pasparakis M, Kollias G, Bruce ME. Tumor necrosis factor alpha-deficient, but not interleukin-6-deficient, mice resist peripheral infection with scrapie. *J Virol* 2000;**74:**3338–3344.
24. Kitamoto T, Shin RW, Doh-ura K, Tomokane N, Miyazono M, Muramoto T, *et al.* Abnormal isoform of prion proteins accumulates in the synaptic structures of the central nervous system in patients with Creutzfeldt-Jakob disease. *Am J Pathol* 1992;**140:**1285–1294.
25. Bell JE, Gentleman SM, Ironside JW, McCardle L, Lantos PL, Doey L, *et al.* Prion protein immunocytochemistry — UK five centre consensus report. *Neuropathol Appl Neurobiol* 1997;**23:**26–35.
26. Wellmann A, Thieblemont C, Pittaluga S, Sakai A, Jaffe ES, Siebert P, *et al.* Detection of differentially expressed genes in lymphomas using cDNA arrays: identification of clusterin as a new diagnostic marker for anaplastic large-cell lymphomas. *Blood* 2000;**96:**398–404.
27. Whipple EC, Shanahan RS, Ditto AH, Taylor RP, Lindorfer MA. Analyses of the in vivo trafficking of stoichiometric doses of an anti-complement receptor 1/2 monoclonal antibody infused intravenously in mice. *J Immunol* 2004;**173:**2297–2306.
28. Mackay F, Browning JL. Turning off follicular dendritic cells. *Nature* 1998;**395:**26–27.
29. Mabbott NA, Bruce ME. Complement component C5 is not involved in scrapie pathogenesis. *Immunobiology* 2004;**209:**545–549.
30. Zlokovic BV. Cerebrovascular transport of Alzheimer's amyloid beta and apolipoproteins J and E: possible anti-amyloidogenic role of the blood-brain barrier. *Life Sci* 1996;**59:**1483–1497.
31. Kempster S, Collins ME, Aronow BJ, Simmons M, Green RB, Edington N. Clusterin shortens the incubation and alters the histopathology of bovine spongiform encephalopathy in mice. *Neuroreport* 2004;**15:**1735–1738.

J Pathol 2006; **209**: 484–491 DOI: 10.1002/path

Journal of Neurochemistry, 2006, **99**, 198–205 doi:10.1111/j.1471-4159.2006.04035.x

Styrylbenzoazole derivatives for imaging of prion plaques and treatment of transmissible spongiform encephalopathies

Kensuke Ishikawa,* Yukitsuka Kudo,† Noriyuki Nishida,‡ Takahiro Suemoto,§ Tohru Sawada,§ Toru Iwaki¶ and Katsumi Doh-ura*

**Department of Prion Research, Tohoku University Graduate School of Medicine, Sendai, Japan*

†Division of Telecommunication and Information Technology, Biomedical Engineering Research Organization, Tohoku University, Sendai, Japan

‡Division of Cellular and Molecular Biology, Nagasaki University Graduate School of Biomedical Sciences, Nagasaki, Japan

§BF Research Institute Inc., Osaka, Japan

¶Department of Neuropathology, Graduate School of Medical Sciences, Kyushu University, Fukuoka, Japan

Abstract

Recent prevalence of acquired forms of transmissible spongiform encephalopathies (TSEs) has urged the development of early diagnostic measures as well as therapeutic interventions. To extend our previous findings on the value of amyloid imaging probes for these purposes, styrylbenzoazole derivatives with better permeability of blood–brain barrier (BBB) were developed and analyzed in this study. The new styrylbenzoazole compounds clearly labeled prion protein (PrP) plaques in brain specimens from human TSE in a manner irrespective of pathogen strain, and a representative compound BF-168 detected abnormal PrP aggregates in the brain of TSE-infected mice when the probe was injected intravenously. On the other hand, most of the compounds inhibited abnormal PrP formation in TSE-infected cells with IC_{50} values in the nanomolar range, indicating that they represent one of the most potent classes of inhibitor ever reported. BF-168 prolonged the lives of mice infected intracerebrally with TSE when the compound was given intravenously at the preclinical stage. The new compounds, however, failed to detect synaptic PrP deposition and to show pathogen-independent therapeutic efficacy, similar to the amyloid imaging probes we previously reported. The compounds were BBB permeable and non-toxic at doses for imaging and treatment; therefore, they are expected to be of practical use in human TSE.

Keywords: amyloid imaging, anti-prion activity, pathogen strain, prion disease, styrylbenzoazole derivatives.

J. Neurochem. (2006) **99**, 198–205.

The transmissible spongiform encephalopathies (TSEs) or prion diseases form a group of neurodegenerative disorders characterized by abnormal deposition of protease-resistant isoforms of prion protein (PrP) in the CNS (Prusiner 1991). TSEs are classified as sporadic, hereditary or environmentally acquired, and have become a serious public health issue because of the recent prevalence of acquired Creutzfeldt–Jakob disease (CJD), such as the variant form due to bovine spongiform encephalopathy (Will *et al.* 1996) and the iatrogenic form with cadaveric growth hormone or dura grafts (Brown *et al.* 2000). There is an urgent need to develop prophylactic and therapeutic interventions as well as diagnostic measures at the preclinical or early clinical stages of these incurable diseases.

We have previously reported that some amyloid imaging compounds, primarily derived from amyloid dyes such as

Received February 16, 2006; revised manuscript received May 25, 2006; accepted May 30, 2006.

Address correspondence and reprint requests to Dr Kensuke Ishikawa, Division of Prion Biology, Department of Prion Research, Tohoku University Graduate School of Medicine, 2–1 Seiryo-machi, Aoba-ku, Sendai 980-8575, Japan. E-mail: ishikawa@mail.tains.tohoku.ac.jp

Abbreviations used: AD, Alzheimer's disease; BBB, blood–brain barrier; BSB, (trans, trans)-1-bromo-2,5-bis-(3-hydroxycarbonyl-4-hydroxy)styrylbenzene; CJD, Creutzfeldt–Jakob disease; DMSO, dimethylsulfoxide; FDDNP, 2-(1-[6-[(2-fluoroethyl)(methyl)amino]-2-naphthyl]ethylidene)malononitrile; GSS, Gerstmann–Strässler–Scheinker syndrome; ICR, Institute of Cancer Research; ID, injected dose; NT, not tested; PrP, prion protein; PrPres, protease-resistant PrP; PTA, phosphotungstic acid; PVDF, polyvinylidene difluoride; TSE, transmissible spongiform encephalopathy.

Congo red and thioflavin T, are useful for detection of prion plaques and treatment of TSE (Ishikawa *et al.* 2004). These compounds, however, are limited in their ability because of inefficient brain uptake. Here we describe new compounds, styrylbenzoazole derivatives, which have been developed for practical use and analyzed for their PrP imaging ability, anti-prion activity, therapeutic efficacy, brain uptake and toxicity.

Materials and methods

Chemicals and experimental models

All of the test compounds were synthesized at Tanabe R & D (Saitama, Japan) and used freshly after being dissolved in 100% dimethylsulfoxide (DMSO).

Cultured cells were grown in Opti-MEM (Invitrogen, Carlsbad, CA, USA) supplemented with 10% fetal calf serum. As cellular models of TSE, we used mouse neuroblastoma (N2a) cells persistently infected with the RML strain (ScN2a) (Race *et al.* 1988) and six other prion-infected cell lines: N2a58 cells individually infected with the RML strain, the 22L strain (Nishida *et al.* 2000) and Fukuoka-1 strain (Ishikawa *et al.* 2004); N2a cells infected with the 22L strain; mouse hypothalamic cells (GT1-7) infected with the 22L strain (Milhavet *et al.* 2000); and mouse fibroblast cells (L929) infected with the RML strain (Vorberg *et al.* 2004).

Tg7 mice overexpressing hamster PrP (Race *et al.* 1995) and Tga20 mice overexpressing mouse PrP (Fischer *et al.* 1996) were also used. These mouse models were intracerebrally infected with 20 μL brain homogenate comprising 1% (w/v) of the 263K strain and the RML strain respectively. The Tg7 mice showed plaque-type PrP deposition between the cerebral cortex and hippocampus by 6 weeks after infection, followed by synaptic-type PrP deposition in the thalamus. The Tga20 mice showed similar pathological deposition, but plaques were not seen as frequently. Each mouse weighed ~30 g, and was maintained under deep ether anesthesia for minimum distress during all surgical procedures. Permission for the animal study was obtained from either the Animal Experiment Committee of Kyushu University or Tohoku University, Japan.

Brain uptake study

Test compounds were administered intravenously to Institute of Cancer Research (ICR) mice under ether anesthesia to determine initial brain uptakes. At 2 or 30 min after injection, the brains were removed, weighed and homogenized with saline. After centrifugation of the homogenate at 21 900 *g* for 10 min, the supernatant was applied to a conditioned C18 solid-phase extraction cartridge, and the compounds were eluted with methyl alcohol. Fluorescence was detected by high performance liquid chromatography with a fluorescence detector as reported previously (Okamura *et al.* 2005), and the percentage of injected dose per gram (%ID/g) was used as a measure of the level of the compounds in the brain.

In vitro PrP imaging in sections

Autopsy-diagnosed brain samples from cases of Gerstmann–Strässler–Scheinker syndrome (GSS) ($n = 2$), sporadic CJD ($n = 5$), iatrogenic dura CJD with synaptic PrP deposition ($n = 1$) and non-TSE control cases with amyloid lesions [Alzheimer's disease (AD), $n = 2$] or without amyloid lesions (cerebral infarction, $n = 1$) were obtained from the Department of Neuropathology, Kyushu University, Japan. After fixation in 10% buffered formalin for 2 weeks, each sample of TSE was immersed in 98% formic acid for the reduction of prion infectivity, embedded in paraffin and cut into sections 7 μm thick. Sections of a variant CJD case were kindly provided by Dr James W. Ironside of the CJD Surveillance Unit, Edinburgh, UK. For neuropathological staining, deparaffinized sections were immersed in 1% Sudan black solution to quench tissue autofluorescence. They were then incubated for 30 min in 1-μM solutions of the test compounds, rinsed with distilled water and examined under a fluorescence microscope (DMRXA; Leica Instruments, Wetzler, Germany) with a UV or FITC filter set.

For comparison, each section was subsequently immunoassayed for PrP as described previously (Doh-ura *et al.* 2000). Briefly, the sections were treated with a hydrolytic autoclave and incubated with a rabbit primary antibody, c-PrP, which was raised against a mouse PrP fragment, amino acids 214–228 (1 : 200; Immuno-Biological Laboratories, Gunma, Japan), followed by incubation with a horseradish peroxidase-conjugated secondary antibody (1 : 200; Vector Laboratories, Burlingame, CA, USA). The reaction product was developed with 3,3′-diaminobenzidine tetrahydrochloride solution and counterstained with hematoxylin. Paraffin-embedded brains of experimental animals were similarly investigated.

In vivo PrP imaging in model animals

BF-168 (molecular weight 312.34) dissolved in 10% DMSO was administered intravenously (0.5–5 mg/kg body weight) into Tg7 mice at 6–7 weeks after injection when the mice showed no apparent clinical signs of TSE. As controls, vehicle alone was similarly injected into infected mice, and BF-168 was administered into uninfected mice. The animals were killed at various time points, and the brains were rapidly frozen and cut into coronal sections 10 μm thick using a cryostat (CM3050; Leica Instruments). The sections were thaw-mounted on slides, dried and coverslipped. They were examined under a fluorescence microscope and further analyzed immunohistochemically as described above.

In vitro treatment in cell cultures

Abnormal PrP formation was assayed by the content of protease-resistant PrP (PrPres) in cellular models of TSE as described previously (Caughey and Raymond 1993). Each compound was added at the designated concentrations when cells were passaged at 10% confluence, while maintaining the final concentration of DMSO in the medium at < 0.5%. The cells were allowed to grow to confluence and lysed with lysis buffer (0.5% sodium deoxycholate, 0.5% Nonidet P-40, phosphate-buffered saline). For analysis of PrPres, samples were digested with 10 μg/mL proteinase K for 30 min, and the digestion was stopped with 0.5 mM phenylmethylsulfonyl fluoride. The samples were centrifuged at 100 000 *g* for 30 min, and pellets were resuspended in 1 × sample loading buffer and boiled. For analysis of cellular PrP in N2a cells, cell lysates were mixed directly with a quarter volume of 5 × sample loading buffer and boiled. These samples were separated by electrophoresis on a 15% Tris–glycine–sodium dodecyl sulfate polyacrylamide gel and electroblotted on to a polyvinylidene difluoride (PVDF) filter (Millipore, Bedford, MA, USA). PrP was detected using a monoclonal antibody, SAF83 (1 : 5000; SPI-BIO, Massy, France), followed by an alkaline phosphatase-conjugated

goat anti-mouse antibody (1 : 20 000; Promega, Madison, WI, USA). Immunoreactive blots were visualized with CDP-Star detection reagent (Amersham, Piscataway, NJ, USA). More than two independent assays were performed in each experiment and signals were analyzed using image analysis software. The approximate concentration of the compound giving 50% inhibition of PrPres formation, relative to the vehicle-treated control (IC_{50}), was estimated by signal intensity. To control for the detection limits of western blotting, we performed additional experiments utilizing sodium phosphotungstic acid (PTA) precipitation, which is the most sensitive technique presently available to detect PrPres (Safar *et al.* 1998). The PTA precipitation was undertaken on cell lysates of ScN2a treated with BF-168 at a designated concentration. The resulting pellets were collected by centrifugation and then analyzed by immunoblotting as described above.

In vivo treatment in model animals

BF-168 solution (4 mg/kg body weight) or vehicle alone was injected intravenously to experimental animals ($n = 5$) once a week. The treatment was started at 2 weeks after injection for Tg7 mice and at 4 weeks after injection for Tga20 mice, and repeated for 4 weeks. A continuous subcutaneous infusion of BF-168 was also given to Tga20 mice ($n = 5$) using an Alzet osmotic pump (Durect, Cupertino, CA, USA). In accordance with the manufacturer's instructions, each pump was filled with BF-168 solution at the designated doses and placed in a subcutaneous area of the back at 4 weeks after injection. The animals showed no apparent adverse effects of the treatment and were monitored 5 days a week until obvious clinical signs appeared. Statistical significance was analyzed by one-way ANOVA followed by Scheffé's method for multiple comparisons.

Results

Brain uptake and toxicity

We designed and synthesized novel styrylbenzoxazole derivatives (Table 1), styrylbenzothiazole and styrylbenzoimidazole derivatives (Table 2) with more efficient permeability of the BBB and less toxicity. Values for brain uptake at 2 min after intravenous injection of the compounds were in the 2.4–17.0%ID/g range, indicating a satisfactory level for imaging probes. Their washouts from the brain varied, with the ratio of %ID/g at 2 min to that at 30 min after injection ranging from 1.0 to 56.9. Acute toxicity was tested by administering each compound intravenously at ~10 mg/kg body weight into normal ICR mice. No apparent toxic effect was observed with any of the compounds tested.

PrP imaging ability

Imaging of abnormal PrP deposition by the compounds was first performed in brain sections of human TSE. The compounds fluorescently labeled most of the PrP plaques in cerebellar cortices of both GSS cases (Fig. 1a, representative data). Among sections from the sporadic CJD cases, PrP deposition was labeled only in a case with plaques (Fig. 1c). In the cerebral cortex from the variant CJD case, large core plaques were detectable, whereas the majority of immunopositive aggregates were not labeled (Fig. 1e). In contrast, no fluorescence signal was identified in sections from the dura CJD case or the other sporadic CJD cases that

Table1 Chemical structure, PrPres inhibition and brain uptake of styrylbenzoxazole derivatives including BF-168

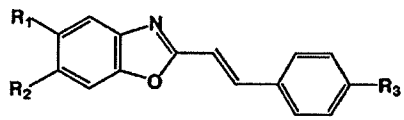

Compound	R_1	R_2	R_3	IC_{50} (nM)[a]	Brain uptake (%ID/g)[b] 2 min	Brain uptake (%ID/g)[b] 30 min	Ratio of 2 to 30 min brain uptake
BF-168	H	$O(CH_2)_2F$	$NH(CH_3)$	0.4	3.9[c]	1.6	2.4
BF-125	H	H	$N(C_2H_5)_2$	10.2	3.0	3.0	1.0
BF-133	F	H	$N(CH_3)_2$	1.6	5.5	3.8	1.4
BF-135	NO_2	H	$N(CH_3)_2$	< 1	NT[d]	NT	-
BF-140	F	H	NH2	< 1	5.5	1.1	5.0
BF-145	F	H	$NH(CH_3)$	< 1	4.4	1.6	2.8
BF-148	H	F	$N(CH_3)_2$	< 1	NT	NT	-
BF-165	H	H	$NH(CH_3)$	7.1	7.2	NT	-
BF-169	H	OH	$NH(CH_3)$	2.4	NT	NT	-
BF-173	I	H	NH_2	2.2	NT	NT	-
BF-180	I	H	$NH(CH_3)$	8.5	2.4	1.8	1.3
BF-191	H	H	Cl	1.8	12.0	1.7	7.1
BF-208	H	H	F	< 1	11.0	0.53	20.8
N-282	H	H	$N(CH_3)_2$	2.1	4.0	1.7	2.4
N-407	H	H	H	< 1	17.0	0.99	17.2

[a]IC_{50}, approximate concentration of a compound giving 50% inhibition of PrPres formation relative to the control in ScN2a cells.
[b]%ID/g, percentage of injected dose per gram in the brains of normal mice.
[c]already reported in the previous work (Okamura *et al.*, 2004).
[d]NT, not tested.

Table 2 Chemical structure, PrPres inhibition and brain uptake of styrylbenzothiazole and styrylbenzoimidazole derivatives

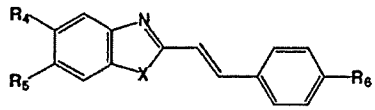

Compound	X	R_4	R_5	R_6	IC_{50} (nM)[a]	Brain uptake (%ID/g)[b] 2 min	Brain uptake (%ID/g)[b] 30 min	Ratio of 2 to 30min brain uptake
BF-124	S	H	H	$N(C_2H_5)_2$	18.1	2.4	2.5	1.0
BF-162	S	F	H	$N(CH_3)_2$	1.4	NT[c]	NT	-
N-276	S	H	H	$N(CH_3)_2$	< 1	NT	NT	-
N-438	S	H	H	H	< 1	11.0	2.0	5.5
BF-126	NH	H	H	$N(C_2H_5)_2$	21	7.2	0.16	45
BF-166	NH	F	H	$N(C_2H_5)_2$	1.1	NT	NT	-
N-457	NH	H	H	Cl	< 1	7.1	0.21	33.8
N-491	NH	H	H	H	1.9	7.4	0.13	56.9

[a]IC_{50}, approximate concentration of a compound giving 50% inhibition of PrPres formation relative to the control in ScN2a cells.
[b]%ID/g, percentage of injected dose per gram in the brains of normal mice.
[c]NT, not tested.

included perivacuolar and/or synaptic PrP deposition (data not shown). Background staining was barely observed after rinsing off the excess compound. Immunohistochemical analysis of PrP revealed that the compounds achieved high-specificity labeling (Figs 1b, d and f). The compounds displayed no signal in control sections without amyloid lesions (data not shown).

Similar results were observed in experimental mice. PrP plaques were specifically labeled in brain sections of Tg7 mice infected with the 263K strain, and there was no PrP immunopositive reaction or fluorescence signal in brain sections of uninfected mice (data not shown). We performed *in vivo* experiments using presymptomatic Tg7 mice at a later stage of TSE. A typical image is shown in Fig. 1(g); peripheral administration of BF-168 fluorescently labeled plaques in the cerebral white matter, indicating that the compound efficiently entered the brain and bound to coarse PrP deposits. Subsequent immunostaining verified the specificity and sensitivity for PrP (Fig. 1h). Non-specific staining, such as cerebrovascular labeling, was occasionally observed at 4 h after injection of 5 mg/kg BF-168, but not after 8 h or more. The stability of the fluorescence signals was examined at various time points up to 24 h after injection and the dye–PrP complex remained visible at the latest time. In contrast, there was no significant labeling after an injection of BF-168 into uninfected animals, or after an injection of vehicle alone to terminally ill Tg7 mice. Similar results were obtained for Tga20 mice infected with the RML strain, although plaques were less frequently detected (data not shown).

Anti-prion activity *in vitro*

The anti-prion activities of the compounds were investigated using ScN2a cells, which are most commonly used for drug screening for TSE treatment. Styrylbenzoxazole derivatives, including BF-168, were evaluated and confirmed to inhibit PrPres formation with IC_{50} values in the nanomolar or subnanomolar range (Fig. 2a and Table 1). Styrylbenzothiazole and styrylbenzoimidazole derivatives were similarly potent, in a dose-dependent manner, within a non-toxic dose range (~10 μM) (Table 2). Treatment with vehicle alone showed no inhibitory effect compared with untreated controls (Fig. 2a). We utilized PTA precipitation, which increases the sensitivity of western blotting, and confirmed the potency of BF-168 at a concentration of 10 times the IC_{50}. Furthermore, radiographic film was exposed to the blotted PVDF membranes for 10 times longer than usual before developing. No significant signals were visualized, whereas bands representing the vehicle-treated control were so strong as to be already saturated (Fig. 2b). To determine whether the efficacy was transient, ScN2a cells treated with 10 nM BF-168 were further cultured for 2 weeks in the absence of BF-168. PrPres signals never reappeared, even through four passages after discontinuation of the treatment (Fig. 2c). To exclude the possibility of interference with immunodetection, BF-168 solution at a final concentration of 10 nM was added to a lysate of untreated ScN2a cells before proteinase K digestion. PrP signals were not affected (data not shown). Nor was any alteration observed in cellular PrP level of N2a cells after treatment with 10 nM BF-168 (Fig. 2d).

To investigate whether the efficacy of the compounds depends on pathogen strain, we tested BF-168 in three N2a58 cell lines individually infected with different strains. As shown in Table 3, BF-168 was only effective in N2a58 cells infected with the RML strain, although the inhibitory activity was not as strong as in ScN2a cells (~1 μM). In contrast, BF-168 was ineffective in the same N2a58 cells infected with the 22L or Fukuoka-1 strains up to 10 μM, a dose at which the compound showed host cytotoxicity.

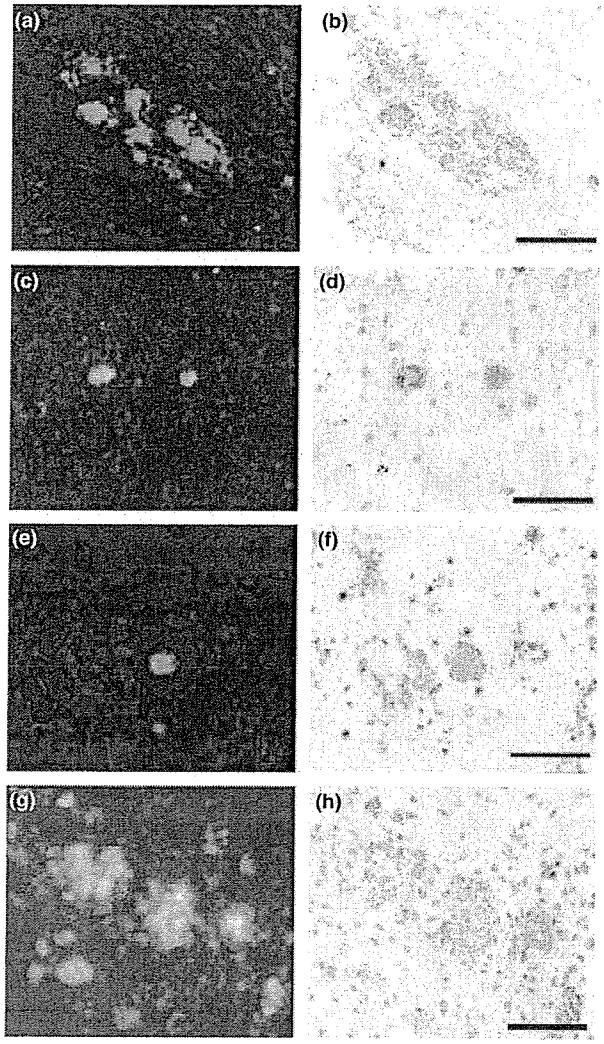

Fig. 1 PrP imaging *in vitro* and *in vivo*. BF-168 fluorescently labeled PrP deposition in a cerebellar section from the case of GSS (a), and in cerebral sections from cases of sporadic CJD with plaques (c) and variant CJD (e). Similar results were obtained from the brains of living TSE-infected mice that were intravenously injected with BF-168 solution (0.5 mg/kg). BF-168 detected PrP deposition in the cerebral white matter between the cortex and hippocampus (g). Sections (a, c, e and g) were subsequently immunoassayed for PrP (b, d, f and h). Bars represent 100 μm (a–f) and 25 μm (g and h).

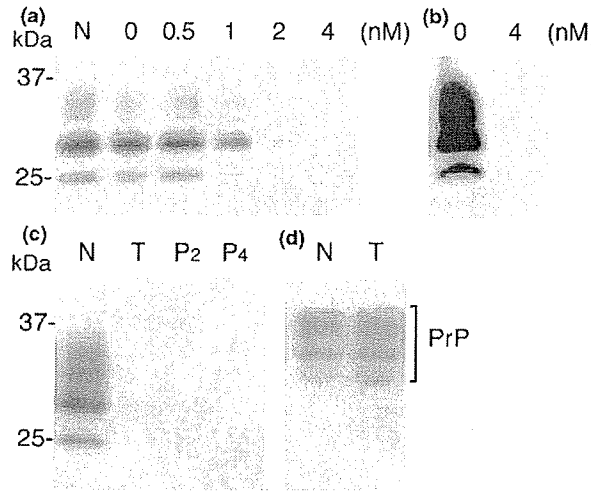

Fig. 2 Effects of BF-168 on PrP expression in ScN2a and N2a cells. BF-168 was added at the designated concentrations to freshly passaged cells. PrPres formation in ScN2a cells was inhibited in a dose-dependent manner (a). To exclude the sensitivity limit of immunoblotting, ScN2a cells treated with 4 nM BF-168 were also analyzed by sodium PTA, and no significant signals were visualized (b). ScN2a cells treated with 10 nM BF-168 were maintained for an additional four passages, and the PrPres signal was not restored in the absence of BF-168 (c). PrP expression was not affected in N2a cells that were grown in the presence of 10 nM BF-168 (d). Lane N, untreated cells; lane 0, cells treated with vehicle alone; lane T, cells treated with 10 nM BF-168; lanes P_2 and P_4, cells following two and four passages after treatment respectively. Bars on the left indicate molecular size markers at 37 and 25 kDa.

Table 3 Anti-prion activities (IC_{50}) of BF-168 in various types of TSE-infected cells

Host cells	Pathogen strains		
	RML	22L	Fukuoka-1
N2a	0.4 nM	None[a]	-[b]
N2a58	~1 μM	None	None
L929	~10 nM	-	-
GT1-7	-	None	-

[a]None, no significant PrPres inhibition up to 10 μM, a dose that affect the rate of cell growth.
[b], not available.

Furthermore, we established L929 cells stably infected with the RML strain. BF-168 inhibited PrPres formation in the RML-infected L929 cells with an IC_{50} in the nanomolar range. We also tested potency against the 22L strain in two other cell lines, N2a and GT1-7 cells. BF-168 was ineffective in either cell line infected with the 22L strain. Other compounds tested here demonstrated similar results (data not shown). These results suggest that the styrylbenzoxazole derivatives exert their inhibitory activity on PrPres formation in a strain-dependent, but not a host cell-dependent, manner.

Therapeutic efficacy *in vivo*

The therapeutic activity of the compounds *in vivo* was assayed in two different mouse models using BF-168 as a representative. Treatment was initiated 2–4 weeks after TSE infection and repeated once a week for 4 weeks. The dosage at a single administration corresponded to a dose sufficient to detect PrP plaques. As shown in Table 4, there was no

Table 4 Effects of BF-168 treatment on intracerebrally TSE-infected mice

Mouse - pathogen strain	*n*	Dose (mg/kg/week)	Administration	Incubation period Mean ± SD (days)
Tg7 - 263K				
	7	Control	-	49.4 ± 1.9
	5	Vehicle	i.v.[a]	50.2 ± 4.1
	5	4	i.v.	52.2 ± 2.6
Tga20 - RML				
	7	Control	-	66.6 ± 1.6
	5	Vehicle	i.v.	64.8 ± 1.6
	5	4	i.v.	72.2 ± 2.5*
	5	10	s.c.[b]	66.0 ± 3.1

* $p < 0.001$ versus the oher groups.
[a]i.V., intravenous injection of BF-168 once a week for 4 weeks from 2 weeks p.i. for Tg7, or 4 weeks p.i. for Tga20.
[b]s.c., continous subcutaneous infusion of BF-168 for 4 weeks from 4 weeks p.i.

significant difference in incubation periods between groups of Tg7 mice infected intracerebrally with the 263K strain, with or without treatment. In contrast, intravenous injection with 4 mg/kg BF-168 significantly prolonged the incubation period (~ 11.4%) of Tga20 mice intracerebrally infected with the RML strain.

In another trial, we used osmotic pumps filled with BF-168 solution, assuming that the route of administration is a key issue. The pump worked continuously for 4 weeks, and the total dosage for the duration was selected to correspond to two to three times that administered intravenously. Subcutaneous infusion of BF-168, however, did not prolong incubation periods of Tga20 mice intracerebrally infected with the RML strain (Table 4). There was no significant difference in incubation period in either group of infected mice between untreated controls and controls treated with vehicle alone.

Discussion

Our results show that styrylbenzoazole derivatives represent candidates for imaging probes as well as therapeutic drugs for TSE. It has been increasingly necessary to develop minimally non-invasive methods for recognizing early clinical infection and evaluating treatment of TSE. We have already focused on two β-amyloid imaging probes and reported them as potential agents for TSE (Ishikawa *et al.* 2004). The problem is, however, that they seemed to have practical limitations because of inadequate brain uptake and washout. Here, we confirmed that novel styrylbenzoazole derivatives clearly labeled PrP plaques *in vitro* and BF-168, the parent compound, entered the brain and labeled PrP plaques *in vivo*, even at a 20-fold lower dose than the probes we previously reported. In brain uptake studies, all of the compounds showed BBB permeability with >1%ID/g, which is proposed to be sufficient for neuroimaging probes. The background staining of 0.5 mg/kg BF-168 was almost absent at 4 h after administration, suggesting excellent clearance from the brain.

Most of styrylbenzoazole derivatives labeled β-amyloid aggregates in AD specimens in this study (data not shown) as well as in the previous study on Alzheimer's (Okamura *et al.* 2004). This is also observed with 2-(1-[6-[(2-fluoroethyl)(methyl)amino]-2-naphthyl]ethylidene)malononitrile (FDDNP), one of the promising agents for imaging β-amyloid deposition. FDDNP has been reported to label PrP plaques in brain sections, and is a candidate for imaging PrP deposition (Bresjanac *et al.* 2003). These findings imply lack of disease specificity, but the compounds should still be useful for some types of TSE, because anatomical distributions of amyloid deposition are characteristically different between diseases. Pathological changes including amyloid deposition of AD brain are always observed in the hippocampus but not in the cerebellum, whereas those of TSE tend to be absent from the hippocampus but to be demonstrated in the cerebellum.

Styrylbenzoazole derivatives detected predominantly PrP plaques, especially in specimens of sporadic CJD with plaques and variant CJD. However, their ability to detect synaptic or perivacuolar PrP deposition remains inconclusive, until more sensitive investigations, such as autoradiography, are available. The compounds tested in this study can be used with radionuclides. ^{18}F-radiolabeled BF-168, which has already been employed for labeling of β-amyloid deposits including both neuritic and diffuse plaques in AD brain (Okamura *et al.* 2004), may be a suitable tool for investigating whether PrP deposition, other than plaque type, can be detected.

This study demonstrated that styrylbenzoazole derivatives have more potent anti-prion activity than the amyloid imaging probes reported previously (Ishikawa *et al.* 2004). Although the neuropathological processes remain unclear, one of the most likely strategies for TSE treatment is a small-molecule drug that can enter the brain and inhibit abnormal PrP formation. It is important to emphasize that styrylbenzoazole derivatives have a wide concentration safety margin, and some were effective even at subnanomolar doses in ScN2a cells. Dozens of drug candidates for TSE have been reported to date but, as far as we know, the most potent inhibitor class for abnormal PrP formation in ScN2a cells is specific blocking antibodies with an IC_{50} in the nanomolar range (Peretz *et al.* 2001).

BF-168 showed no apparent alteration in cellular PrP expression level in N2a cells, and also labeled abnormal PrP deposition both *in vitro* and *in vivo*. These data suggest that styrylbenzoazole derivatives might interact directly with abnormal PrP molecules to block the conversion of normal to abnormal PrP. The structure–activity relationship, examined by introducing side-chain or functional groups into the benzoazole and/or benzene rings, demonstrates that the inhibitory potency is not always the same, even among

closely related compounds (data not shown). Although we could not obtain any insight into inhibitory mechanisms, the efficacy of BF-168 was dependent on pathogen strain, and this is consistent with our previous work using three types of cell lines (Ishikawa *et al.* 2004). In an attempt to further explore strain dependency, we tested three different pathogen strains in one host cell line, and three different host cell lines with one pathogen strain. BF-168 inhibited abnormal PrP formation in all three types of RML-infected cells, including ScN2a cells. By contrast, BF-168 did not demonstrate any inhibitory activity in the 22L- or Fukuoka-1-infected cells. It is well known that prion strains differ in their biological profiles such as the degree of glycosylation and the conformation of PrP molecules. In the imaging experiments we confirmed that the compound bound to a certain type of abnormal PrP aggregates. Thus, it was assumed that the therapeutic efficacy might be based on blocking certain interactions between normal and abnormal PrP, and that BF-168 might recognize the PrP conformation. However, considering a discrepancy in the *in vivo* experiment between PrP imaging and treatment using infected Tg7 mice, these inferences remain unsupported and the precise mechanism of the strain-dependent efficacies needs to be elucidated.

Kocisko *et al.* (2004) reported that anti-prion activity *in vitro* does not always correlate with that *in vivo*. With *in vivo* testing, there are many variables, such as inoculation route, dosing protocol and pathogen strain. The efficacy differed according to the BF-168 administration route in Tga20 mice, even though the dose administered subcutaneously for the same duration was no less than that administered intravenously. This might be due to differences in stability and clearance of BF-168 in relation to the route of administration.

Most previous therapeutic investigations showed a significant benefit *in vivo* when the treatment was started before, or soon after, peripheral TSE infection. Although the efficacy of BF-168 was limited, it is noteworthy that we obtained significant results with peripheral administration at a later stage of the intracerebral infection. In addition, BF-168 showed excellent brain uptake and binding affinity towards PrP aggregates *in vivo*, even at a low dose, suggesting that the compound should be a good imaging probe for clinical use. In the treatment of infected Tga20 mice, BF-168 showed almost the same prolongation of the incubation period but with a 10-fold smaller dose than (trans, trans)-1-bromo-2,5-bis-(3-hydroxycarbonyl-4-hydroxy)styrylbenzene (BSB), which we reported previously as one of the amyloid imaging probes applicable for TSE (Ishikawa *et al.* 2004). BF-168 showed a low IC_{50} of 0.4 nM in treatment of ScN2a cells, whereas the IC_{50} of BSB was more than 1000-fold higher (1.4 μM). We decided the dosing protocol for our experimental animals from *in vitro* data, including the ratio of these IC_{50} values, and from an *invivo* imaging experiment in which 0.1 mg BF-168 per injection was enough to detect PrP deposition. It is also necessary to consider washout of the compound from the brain. Further studies are required to examine issues such as dose–response relationships, administration time and dosing conditions. Furthermore, there was a problem in that administration frequency was limited because animal tail tissue was damaged by repetitive intravenous injections. In addition, it should be investigated whether compounds with slower washout from the brain are more suitable as therapeutic agents.

In conclusion, styrylbenzoazole derivatives efficiently entered the brain and labeled pathological PrP deposition, and demonstrated some anti-prion activities both *in vitro* and *in vivo*. Although their efficacy depended on the pathogen strain, these are a new class of compounds with potential as therapeutic drugs and imaging probes for TSE.

Acknowledgements

This study was supported by grants to KD from the Ministry of Health, Labour and Welfare (H16-kokoro-024) and the Ministry of Education, Culture, Sports, Science and Technology 13557118, 14021085, Japan. The authors thank Dr James W. Ironside of the CJD Surveillance Unit, Edinburgh, UK, for providing the variant CJD specimens.

References

Bresjanac M., Smid L. M., Vovko T. D., Petric A., Barrio J. R. and Popovic M. (2003) Molecular-imaging probe 2-(1-[6-[(2-fluoroethyl)(methyl) amino]-2-naphthyl]ethylidene) malononitrile labels prion plaques *in vitro*. *J. Neurosci.* **23**, 8029–8033.

Brown P., Preece M., Brandel J. P. *et al.* (2000) Iatrogenic Creutzfeldt–Jakob disease at the millennium. *Neurology* **55**, 1075–1081.

Caughey B. and Raymond G. J. (1993) Sulfated polyanion inhibition of scrapie-associated PrP accumulation in cultured cells. *J. Virol.* **67**, 643–650.

Doh-ura K., Mekada E., Ogomori K. and Iwaki T. (2000) Enhanced CD9 expression in the mouse and human brains infected with transmissible spongiform encephalopathies. *J. Neuropathol. Exp. Neurol.* **59**, 774–785.

Fischer M., Rulicke T., Raeber A., Sailer A., Moser M., Oesch B., Brandner S., Aguzzi A. and Weissmann C. (1996) Prion protein (PrP) with amino-proximal deletions restoring susceptibility of PrP knockout mice to scrapie. *EMBO J.* **15**, 1255–1264.

Ishikawa K., Doh-ura K., Kudo Y., Nishida N., Murakami-Kubo I., Ando Y., Sawada T. and Iwaki T. (2004) Amyloid imaging probes are useful for detection of prion plaques and treatment of transmissible spongiform encephalopathies. *J. Gen. Virol.* **85**, 1785–1790.

Kocisko D. A., Morrey J. D., Race R. E., Chen J. and Caughey B. (2004) Evaluation of new cell culture inhibitors of protease-resistant prion protein against scrapie infection in mice. *J. Gen. Virol.* **85**, 2479–2483.

Milhavet O., McMahon H. E., Rachidi W. *et al.* (2000) Prion infection impairs the cellular response to oxidative stress. *Proc. Natl Acad. Sci. USA* **97**, 13 937–13 942.

Nishida N., Harris D. A., Vilette D., Laude H., Frobert Y., Grassi J., Casanova D., Milhavet O. and Lehmann S. (2000) Successful transmission of three mouse-adapted scrapie strains to murine neuroblastoma cell lines overexpressing wild-type mouse prion protein. *J. Virol.* **74**, 320–325.

Okamura N., Suemoto T., Shimadzu H. *et al.* (2004) Styrylbenzoxazole derivatives for *in vivo* imaging of amyloid plaques in the brain. *J. Neurosci.* **24**, 2535–2541.

Okamura N., Suemoto T., Furumoto S. *et al.* (2005) Quinoline and benzimidazole derivatives: candidate probes for *in vivo* imaging of tau pathology in Alzheimer's disease. *J. Neurosci.* **25**, 10 857–10 862.

Peretz D., Williamson R. A., Kaneko K. *et al.* (2001) Antibodies inhibit prion propagation and clear cell cultures of prion infectivity. *Nature* **412**, 739–743.

Prusiner S. B. (1991) Molecular biology of prion diseases. *Science* **252**, 1515–1522.

Race R. E., Caughey B., Graham K., Ernst D. and Chesebro B. (1988) Analyses of frequency of infection, specific infectivity, and prion protein biosynthesis in scrapie-infected neuroblastoma cell clones. *J. Virol.* **62**, 2845–2849.

Race R. E., Priola S. A., Bessen R. A., Ernst D., Dockter J., Rall G. F., Mucke L., Chesebro B. and Oldstone M. B. (1995) Neuron-specific expression of a hamster prion protein minigene in transgenic mice induces susceptibility to hamster scrapie agent. *Neuron* **15**, 1183–1191.

Safar J., Wille H., Itri V., Groth D., Serban H., Torchia M., Cohen F. E. and Prusiner S. B. (1998) Eight prion strains have PrP(Sc) molecules with different conformations. *Nat. Med.* **4**, 1157–1165.

Vorberg I., Raines A., Story B. and Priola S. A. (2004) Susceptibility of common fibroblast cell lines to transmissible spongiform encephalopathy agents. *J. Infect. Dis.* **189**, 431–439.

Will R. G., Ironside J. W., Zeidler M. *et al.* (1996) A new variant of Creutzfeldt–Jakob disease in the UK. *Lancet* **347**, 921–925.

Available online at www.sciencedirect.com
ScienceDirect
Bioorganic & Medicinal Chemistry Letters
ELSEVIER
Bioorganic & Medicinal Chemistry Letters 16 (2006) 5982–5987

Metal complexes with superoxide dismutase-like activity as candidates for anti-prion drug

Tomoko Fukuuchi,[a,b,*] Katsumi Doh-ura,[c] Shin'ichi Yoshihara[b] and Shigeru Ohta[a]

[a]*Graduate School of Biomedical Sciences, Hiroshima University, 1-2-3 Kasumi, Minami-ku, Hiroshima 734-8553, Japan*
[b]*Faculty of Pharmaceutical Sciences, Hiroshima International University, 5-1-1 Koshingai, Hiro, Kure, Hiroshima 737-0112, Japan*
[c]*Graduate School of Medicine, Tohoku University, 2-1 Seiryo-cho, Aoba-ku, Sendai 980-8575, Japan*

Received 28 July 2006; revised 29 August 2006; accepted 30 August 2006
Available online 20 September 2006

Abstract—Various compounds were evaluated for ability to inhibit the formation of the abnormal protease-resistant form of prion protein (PrP-res) in two cell lines infected with different prion strains. Examination of the structure–activity relationships indicated that compounds with copper-selective chelating ability and whose copper complexes have high SOD-like activity are candidates for anti-prion drug.

Transmissible spongiform encephalophathies (TSEs) or prion diseases are a group of fatal neurodegenerative disorders, and their development is associated with accumulation of aggregated proteins, oxidative damage to the brain, and neuronal cell loss. Prion diseases are characterized by the generation of a protein molecule termed PrP^{Sc} (scrapie isoform of the prion protein), which is a conformational variant of the normal host protein, PrP^{C} (cellular isoform of the prion protein).[1,2] It is believed that the conversion of PrP^{C} into PrP^{Sc} is the key event in the pathogenesis of TSEs.

The octapeptide repeat region of the PrP^{C} binds several copper ions with concentration of the micromolar range[3,4] and their dissociation constant for the ion is reported to be femtomolar range.[5] The biological significance of this interaction is not clear, but it is reported that PrP^{C} has a copper-dependent superoxide dismutase (SOD) activity[6] and PrP^{C} may be involved in copper uptake into cells.[7,8] Recently, there has been increasing interest in the role of metal ions, in particular copper, in prion diseases.[9,10]

In the early 1970s, it was reported that the copper chelator cuprizone induced prion diseases-like histopathological changes in mice.[11,12] On the other hand, Sigurdsson et al. recently found that a copper chelator, D-penicillamine, delayed the onset of prion disease in infected mice, and suggested that chelator-based therapy might attenuate the disease.[13] Copper has been implicated in the pathogenesis of prion disease, but numerous studies have only succeeded in demonstrating the complexity of the effects of copper on the development of prion diseases, and it remains unclear whether this ion promotes or inhibits disease progression.

In the present study, we evaluated the ability of a wide range of compounds[14] to inhibit the formation of the abnormal protease-resistant form of prion protein (PrP-res), using two cell lines, ScN2a cells and F3, infected with different prion strains.[15,16] We then analyzed the structure–activity relationships to investigate what kinds of structure or biochemical characteristics contribute to anti-prion activity.

Spectrophotometric complexation studies.[17–19] The complexes were prepared as previously reported.[20,21] Solutions of 10 mM $Cu(ClO_4)_2$ and 8-hydroxyquinoline were prepared in H_2O. Cu(II)-chelate formation of 8-hydroxyquinoline was demonstrated by Job's method.[18,19] The spectrophotometric complexation studies showed that 8-hydroxyquinoline binds in 2:1 ratio with Cu(II) (Fig. 1A). 2,2′-Biquinoline, neocuproine, bathocuproine, 4,4′-dicarboxy-2,2′-biquinoline, porphyrins, cimetidine and D-penicillamine bind in 1:1 ratio with Cu(II) (2,2′-biquinoline, Fig. 1B; others, data not

Keywords: Prion; 2,2′-Biquinoline; Cimetidine; TPEN; Copper; Chelate; Metal complex; SOD activity.
* Corresponding author. Tel./fax: +81 823 73 8573; e-mail: t-fukuu@ps.hirokoku-u.ac.jp

0960-894X/$ - see front matter © 2006 Elsevier Ltd. All rights reserved.
doi:10.1016/j.bmcl.2006.08.115

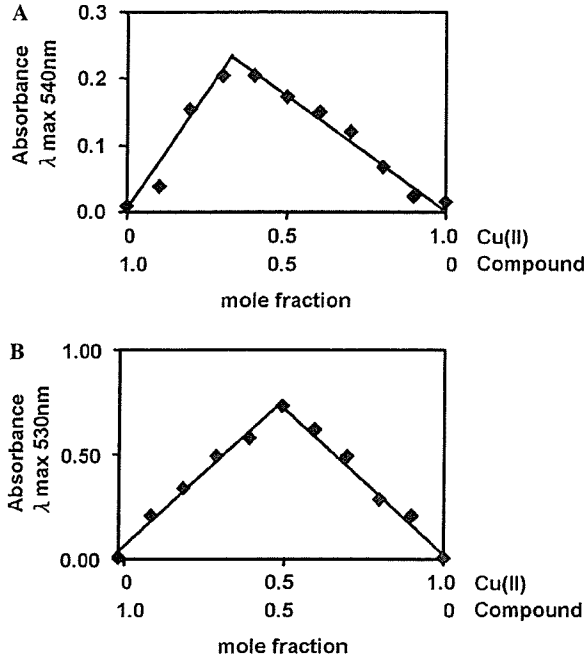

Figure 1. Continuous variation plots for 8-hydroxyquinoline and Cu(II) (A) and 2,2′-biquinoline and Cu(II) (B). (A) 2:1 binding ratio between 8-hydroxyquinoline and Cu(II), (B) 1:1 binding ratio between 2,2′-biquinoline and Cu(II). The plots were obtained by Job's method in aqueous solution.

shown). However, it has been reported that the oxidation state of copper may be altered in the D-penicillamine complex, and the complex prepared in this way contains both Cu(I) and Cu(II).[22]

Inhibition of PrP-res formation in ScN2a cells and F3 cells by metal chelators.[23–26] 1,10-Phenanthroline, 2,2′,2″-terpyridine and 8-hydroxyquinoline did not inhibit PrP-res formation within a nontoxic dose range (Table 1), but were cytotoxic at 100 nM. Chelators of this class can chelate a wide variety of metals.

Neocuproine, bathocuproine, 2,2′-biquinoline and 4,4′-dicarboxy-2,2′-biquinoline are highly specific copper chelators. The chelators of this class, except 4,4′-dicarboxy-2,2′-biquinoline, effectively inhibited PrP-res formation in ScN2a cells and F3 cells in a dose-dependent manner (Fig. 2). The concentrations giving 50% inhibition (IC_{50}) of PrP-res formation in ScN2a cells relative to the DMSO-treated or untreated control ranged from 5 to 80 nM (Table 1). These compounds showed no apparent cytotoxicity at concentrations up to 1 μM. However, neocuproine was ineffective in F3 cells within a nontoxic dose range. Findings from these experiments suggest that compounds having copper-selective chelating ability are more effective inhibitors than non-selective metal-chelating compounds, but not an exclusive factor.

Inhibition of PrP-res formation in ScN2a cells and F3 cells by porphyrins.[23–26] Porphyrins can form 1:1 stable chelates with various metal ions. The order of stability for divalent metal ions is Cu > Fe > Zn > Mn, regardless of the type of substituents on the porphyrin ring. Porphyrins were effective inhibitors of PrP-res formation, with IC_{50} values ranging from 5 to 320 nM in ScN2a cells and F3 cells (Table 2). And Mn(III)–porphyrins complexes showed higher anti-prion activity than the metal-free compounds (Table 2).

SOD-like activity and correlation with anti-prion activity. It is known that Mn(III)–porphyrin complexes show high SOD-like activity in vitro and in vivo.[27,28] We thought that SOD-like activity might contribute to the anti-prion activity of such compounds, since the SOD activity of PrP^C is decreased by conversion to PrP^{Sc}. Therefore, we focused on chelators having SOD-like activity. Many low-molecular metal complexes, mainly copper, manganese and iron complexes, have been synthesized and their SOD-like activity examined in vitro and in vivo,[29–33] and some of them showed activity in vivo.[34–36] As shown in Table 3, SOD-like activity of these compounds was measured in vitro by our methods.[37] The SOD-like activity in cell lysates was significantly increased when these metal-free compounds were added to the cell cultures (data not shown). Therefore, the chelators that showed anti-prion activity formed metal complexes and had SOD-like activity.

Among these compounds, we chose cimetidine[34,38] and TPEN[39] for further examination, as well as Mn-TCPP (Mn-TBAP), which we had already examined. Cimetidine effectively inhibited PrP-res formation, with IC_{50} values of 5 nM in ScN2a cells and 200 nM in F3 cells. TPEN inhibited PrP-res formation, with IC_{50} values of 5 nM in ScN2a cells and 200 nM in F3 cells.

We found that the compounds, shown in Tables 1 and 2, with higher anti-prion activity in ScN2a cells had higher SOD-like activity (Table 3). Statistical analysis exhibited a significant linear correlation between these two activities ($r = 0.93$) (Fig. 3).

Despite numerous studies, it remains unclear whether copper ions promote[13] or inhibit[40] prion disease. In Alzheimer's disease, another neurodegenerative disease, the copper- and zinc-selective chelator clioquinol was effective in decreasing β-amyloid deposits.[41] However, Doh-ura et al. found that clioquinol and related compounds, quinoline hydrochloride, 8-hydroxyquinoline, and 8-acetoxyquinoline, were ineffective in scrapie-infected mouse neuroblastoma (ScNB) cells.[25] Thus, chelating drugs that are effective in inhibiting β-amyloid formation may not inhibit the conversion of PrP^C to PrP^{Sc}.

In this study, we evaluated the anti-prion activity of various compounds having metal-chelating ability in order to identify the requirements for anti-prion activity. We found that many, but not all, compounds having selective copper-chelating ability are effective inhibitors of PrP-res formation in ScN2a cells and F3 cells. Thus, copper-selective chelating ability per se may not be essential for anti-prion activity. This idea is supported by the observation that porphyrins chelating manganese

Table 1. Inhibition of PrP-res formation in ScN2a cells and F3 cells by metal chelators

Compound	Structure	Metal(M)	Inhibition PrP-res IC_{50} (nM)	
			ScN2a cells	F3 cells
1,10-Phenanthroline	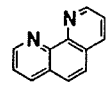		N.E.	N.E.
2,2′,2″-Terpyridine	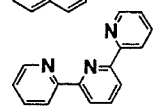		N.E.	N.E.
8-Hydroxyquinoline			N.E.	N.E.
Bis(8-quinolinolato) Copper(II)		Cu^{2+}	N.E.	N.E.
Bis(8-quinolinolato) Zinc(II)		Zn^{2+}	N.E.	N.E.
Neocuproine	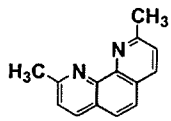		80	N.E.
Bathocuproine	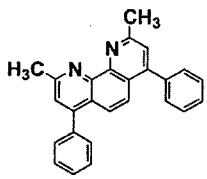		80	200
2,2′-Biquinoline	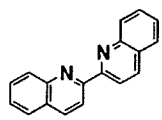		5	250
4,4′-Dicarboxy-2,2′-biquinoline	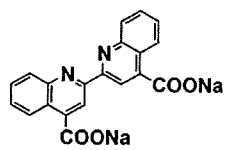		N.E.	N.E.

N.E., no effect.
IC_{50}, concentration of a compound causing 50% inhibition of PrP-res formation relative to the control.

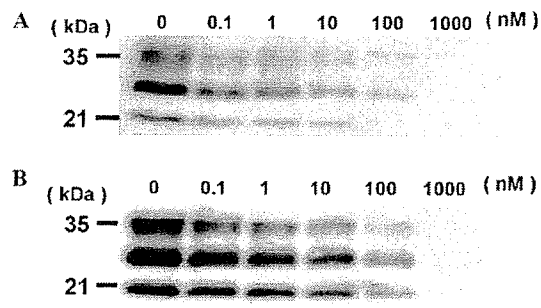

Figure 2. Anti-prion activity of 2,2′-biquinoline in prion-infected cells. Various concentrations of the compound were added to freshly passaged ScN2a cells (A) or F3 cells (B), and the PrP-res levels were analyzed by Western blotting. Lanes: 0, cells treated with DMSO alone; others, treated with the indicated concentration of 2,2′-biquinoline. Bars on the left indicate molecular mass markers at 35 and 21 kDa.

showed greater anti-prion activity than the metal-free compounds. Therefore, we examined whether SOD-like activity was associated with anti-prion activity, and discovered that this was the case.

PrP^C plays an important role in cell protection from oxidative stress, and modulates the activity of antioxidant enzymes by regulating the intracellular copper concentration, but it can also play a direct role owing to its intrinsic SOD activity.[6,42,43] Cells with accumulated abnormal PrP^{Sc} displayed the phenotypes of decreased copper-binding capacity and higher sensitivity to oxidative stress.[16,44] Interestingly, we found a significant correlation ($r = 0.93$) between SOD-like activity and anti-prion activity. Furthermore, we confirmed that the copper complex of D-penicillamine, which has been reported

Table 2. Inhibition of PrP-res formation in ScN2a cells and F3 cells by porphyrins

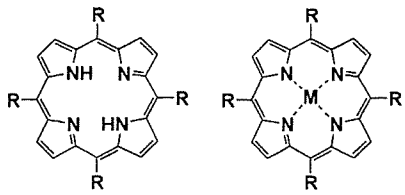

Compound	R	Metal(M)	Inhibition PrP-res IC_{50} (nM)	
			ScN2a cells	F3 cells
TPP			10	320
TCPP	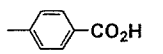		250	160
Mn-TCPP (MnTBAP)	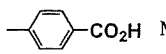	Mn^{3+}	40	60
TPPS	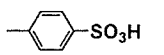		200	160
TMPyP	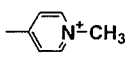		130	160
Mn-TMPyP	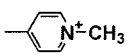	Mn^{3+}	5	40

IC_{50}, concentration of a compound giving 50% inhibition of PrP-res formation relative to the control.

Table 3. SOD-like activity of metal complexes

Chelating metal	Compound	SOD-like activity IC_{50} (μM)
Cu	8-Hydroxyquinoline	263
	Clioquinol	140
	Neocuproine	50
	Bathocuproine	32
	2,2′-Biquinoline	3
	4,4′-Dicarboxy-2,2′-biquinoline	263
	Cimetidine	0.4
	D-Penicillamine	28
Mn	TCPP	8
	TMPyP	0.3
Fe	TPEN	0.4

IC_{50}, concentration of a compound giving 50% inhibition of WST-1 reduction.

to show anti-prion activity, exhibits SOD-like activity.[13]

It is not easy to find molecules with both good metal-binding ability and high SOD-like activity, because, taking copper ions as an example, the former property means the Cu(II) complex is rather stable, while the latter property implies that the complex is prone to be reduced to the Cu(I)-chelator state.[45] This might explain why compounds such as clioquinol that are good copper chelators are nevertheless ineffective in terms of anti-prion activity.[25]

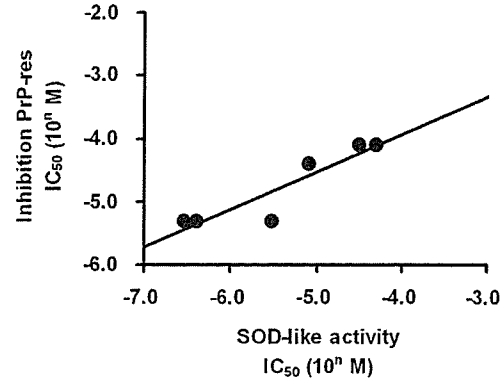

Figure 3. Correlation between SOD-like activity and inhibition of PrP-res formation in ScN2a cells. The plot shows data from seven compounds for which both SOD activity and inhibition of PrP-res formation were determined. ($r = 0.93$) SOD-like activity IC_{50}: concentration of a compound giving 50% inhibition of WST-1 reduction. Inhibition PrP-res IC_{50}: concentration of a compound giving 50% inhibition of PrP-res formation relative to the control.

On the other hand, cimetidine can form complexes with both Cu(I) and Cu(II), and has satisfactory SOD-like activity in both states, so it may be a good candidate for anti-prion activity. Furthermore, cimetidine can cross the blood–brain barrier to act in the central nerve system.[46] This type of compounds may provide a possible therapeutic approach for prion diseases.

In conclusion, we suggest that compounds which have copper-selective chelating ability, and whose copper complexes have high SOD-like activity are candidates for anti-prion drug.

References and notes

1. Prusiner, S. B. *Science* **1982**, *216*, 136.
2. Bounias, M.; Purdey, M. *Sci. Total Environ.* **2002**, *297*, 1.
3. Brown, D. R.; Qin, K.; Herms, J. W.; Madlung, A.; Manson, J.; Strome, R.; Fraser, P. E.; Kruck, T.; von Bohlen, A.; Schulz-Schaeffer, W.; Giese, A.; Westaway, D.; Kretzschmar, H. *Nature* **1997**, *390*, 684.
4. Viles, J. H.; Cohen, F. E.; Prusiner, S. B.; Goodin, D. B.; Wright, P. E.; Dyson, H. J. *Proc. Natl. Acad. Sci. U.S.A.* **1999**, *96*, 2042.
5. Jackson, G. S.; Murray, I.; Hosszu, L. L.; Gibbs, N.; Waltho, J. P.; Clarke, A. R.; Collinge, J. *Proc. Natl. Acad. Sci. U.S.A.* **2001**, *98*, 8531.
6. Brown, D. R.; Wong, B. S.; Hafiz, F.; Clive, C.; Haswell, S. J.; Jones, I. M. *Biochem. J.* **1999**, *344*, 1.
7. Brown, D. R. *J. Neurosci. Res.* **1999**, *58*, 717.
8. Pauly, P. C.; Harris, D. A. *J. Biol. Chem.* **1998**, *273*, 33107.

9. McKenzie, D.; Bartz, J.; Mirwald, J.; Olander, D.; Marsh, R.; Aiken, J. *J. Biol. Chem.* **1998**, *273*, 25545.
10. Brown, D. R.; Hafiz, F.; Glass-smith, L. L.; Wong, B. S.; Jones, I. M.; Clive, C.; Haswell, S. J. *EMBO J.* **2000**, *19*, 1180.
11. Kimberlin, R. H.; Millson, G. C.; Bountiff, L.; Collis, S. C. *J. Comp. Pathol.* **1974**, *84*, 263.
12. Pattison, I. H.; Jebbett, J. N. *Nature* **1971**, *230*, 115.
13. Sigurdsson, E. M.; Brown, D. R.; Alim, M. A.; Scholtzova, H.; Carp, R.; Meeker, H. C.; Prelli, F.; Frangione, B.; Wisniewski, T. *J. Biol. Chem.* **2003**, *278*, 46199.
14. Copper(II) perchlorate hexahydrate 98% and D-penicillamine were purchased from Sigma. Iron(II) sulfate heptahydrate, 2,2′-biquinoline, and cimetidine were purchased from Wako Pure Chemical (Osaka, Japan). 1,10-Phenanthroline monohydrate, 2,9-dimethyl-4,7-dimethyl-1,10-phenanthroline (bathocuproine), 2,9-1,10-phenanthroline (neocuproine), tetraphenylporphine (TPP), tetraphenylporphine tetrasulfonic acid (TPPS), α,β,γ,δ-tetrakis(1-methylpyridinium-4-yl)porphine *p*-toluenesulfonate (TMPyP), tetrakis(4-carboxyphenyl)porphine (TCPP), 2,2′-bicinchoninic acid dipotassium salt, 5-chloro-7-iodo-8-hydroxyquinoline (clioquinol), and 8-hydroxyquinoline were purchased from Tokyo Kasei (Tokyo, Japan). Manganese(III) tetrakis(1-methylpyridinium-4-yl)porphyrin pentachloride (Mn-TMPyP) and Mn(III)tetrakis(4-benzoic acid)porphyrin chloride(Mn-TCPP or Mn-TBAP) were purchased from Calbiochem (California, USA). They were dissolved in 100% dimethylsulfoxide (DMSO) or 95% ethanol just before use.
15. Two types of prion-infected mouse neuroblastoma (N2a) cell lines were used in this study: N2a cells infected with the RML strain (ScN2a) [16] and N2a#58 cells infected with the Fukuoka-1 strain (F3). N2a#58 cells are known to express five times more normal PrP than N2a cells. Both ScN2a cells and F3 cells were grown in six-well culture plates in Opti-MEM (Invitrogen) supplemented with 10% fetal bovine serum. The cells were allowed to reach confluence, and chemicals at various concentrations were added to the medium when 5% of the confluent cells were passaged.The final concentration of either DMSO or ethanol in the medium was less than 0.2%. The cultures were allowed to grow to confluence (3 or 4 days).
16. Milhavet, O.; McMahon, H. E.; Rachidi, W.; Nishida, N.; Katamine, S.; Mange, A.; Arlotto, M.; Casanova, D.; Riondel, J.; Favier, A.; Lehmann, S. *Proc. Natl. Acad. Sci. U.S.A.* **2000**, *97*, 13937.
17. The chelation study was carried out using Job's method.[18,19] Solutions of 10 mM Cu(II) and each compound at a compound:Cu (II) ratio of 1:0 to 0:1 were prepared in ultrapure water (MilliQ; Millipore Co., Japan) or 95% ethanol, and λmax of the copper complex was measured.
18. Vosburgh, W. C.; Cooper, G. R. *J. Am. Chem. Soc.* **1941**, *63*, 437.
19. Job, P. *Ann. Chim.* **1928**, *9*, 113.
20. Kolthoff, I. M. S.; Sandell, E. B. *Textbook of Quantitative Inorganic Analysis*; Pergamon Press: New York, 1959, The MacMillan Co.
21. Ueno, K.; Imamura, T.; Cheng, K. L. *Handbook of Organic Analytical Reagents*; Pergamon Press: Tokyo, 1992, CRC Press.
22. Birker, P. J.; Freeman, H. C. *J. Am. Chem. Soc.* **1977**, *99*, 6890.
23. The anti-prion activity of each compound was assayed by measuring the 50%-inhibitory concentration (IC_{50}) for PrP-res formation in ScN2a cells and F3 cells, as described in previous reports.[24–26] Briefly, compounds were added at designated concentrations to the medium when cells were passaged at 10% confluency. The cells were allowed to grow to confluence and lysed with lysis buffer (0.5% sodium deoxycholate, 0.5% Nonidet P-40, and PBS). The lysates were digested with 10 μg/ml proteinase K for 30 min at 37 °C and centrifuged at 15,000 rpm for 5 min at 24 °C with GLASSFOG(Q-bio gene, USA). The pellets were resuspended in sample loading buffer and boiled. Samples were separated by electrophoresis on 15% Tris–glycine–SDS–polyacrylamide gel and electroblotted. PrP-res was detected using an antibody, SAF83 (1:5000; SPI-Bio, France), followed by an alkaline phosphatase-conjugated secondary antibody. Immunoreactive signals were visualized using CDP-Star detection reagent (Amersham Biosciences Corp., U.S.A.) and were analyzed densitometrically. At least three independent experiments were performed to estimate IC_{50} of each compound.
24. Doh-Ura, K.; Iwaki, T.; Caughey, B. *J. Virol.* **2000**, *74*, 4894.
25. Murakami-Kubo, I.; Doh-ura, K.; Ishikawa, K.; Kawatake, S.; Sasaki, K.; Kira, J.; Ohta, S.; Iwaki, T. *J. Virol.* **2004**, *78*, 1281.
26. Ishikawa, K.; Doh-ura, K.; Kudo, Y.; Nishida, N.; Murakami-Kubo, I.; Ando, Y.; Sawada, T.; Iwaki, T. *J. Gen. Virol.* **2004**, *85*, 1785.
27. Day, B. J.; Shawen, S.; Liochev, S. I.; Crapo, J. D. *J. Pharmacol. Exp. Ther.* **1995**, *275*, 1227.
28. Day, B. J.; Crapo, J. D. *Toxicol. Appl. Pharmacol.* **1996**, *140*, 94.
29. Younes, M.; Lengfelder, E.; Zienau, S.; Weser, U. *Biochem. Biophys. Res. Commun.* **1978**, *81*, 576.
30. Kimura, E.; Sakonaka, A.; Nakamoto, M. *Biochim. Biophys. Acta* **1981**, *678*, 172.
31. Kimura, E.; Yatsunami, A.; Watanabe, A.; Machida, R.; Koike, T.; Fujioka, H.; Kuramoto, Y.; Sumomogi, M.; Kunimitsu, K.; Yamashita, A. *Biochim. Biophys. Acta* **1983**, *745*, 37.
32. Wada, K.; Fujibayashi, Y.; Yokoyama, A. *Arch. Biochem. Biophys.* **1994**, *310*, 1.
33. Goldstein, S.; Czapski, G. *Free Radic. Res. Commun.* **1991**, *12–13*, 205.
34. Baudry, M.; Etienne, S.; Bruce, A.; Palucki, M.; Jacobsen, E.; Malfroy, B. *Biochem. Biophys. Res. Commun.* **1993**, *192*, 964.
35. Darr, D. J.; Yanni, S.; Pinnell, S. R. *Free Radic. Biol. Med.* **1988**, *4*, 357.
36. Wada, K.; Fujibayashi, Y.; Tajima, N.; Yokoyama, A. *Biol. Pharm. Bull.* **1994**, *17*, 701.
37. SOD-like assay kit-WST (Dojindo Chemical, Kumamoto, Japan) was used for the quantification of SOD-like activity. This method is a xanthine-based spectrophotometric assay using the tetrazolium salt WST-1. The SOD-like activity was evaluated using the standard curve of SOD-like activity versus absorbance at 450 nm. Differences of SOD-like activity were tested by use of the unpaired Student's *t* test, and *p* values smaller than 0.05 were considered to be statistically significant.
38. Kimura, E.; Koike, T.; Shimizu, Y.; Kodama, M. *Inorg. Chem.* **1986**, *25*, 2242.
39. Nagano, T.; Hirano, T.; Hirobe, M. *J. Biol. Chem.* **1989**, *264*, 9243.
40. Hijazi, N.; Shaked, Y.; Rosenmann, H.; Ben-Hur, T.; Gabizon, R. *Brain Res.* **2003**, *993*, 192.
41. Cherny, R. A.; Atwood, C. S.; Xilinas, M. E.; Gray, D. N.; Jones, W. D.; McLean, C. A.; Barnham, K. J.; Volitakis, I.; Fraser, F. W.; Kim, Y.; Huang, X.; Goldstein, L. E.; Moir, R. D.; Lim, J. T.; Beyreuther, K.;

Zheng, H.; Tanzi, R. E.; Masters, C. L.; Bush, A. I. *Neuron* **2001**, *30*, 665.
42. Martins, V. R.; Mercadante, A. F.; Cabral, A. L.; Freitas, A. R.; Castro, R. M. *Braz. J. Med. Biol. Res.* **2001**, *34*, 585.
43. Rachidi, W.; Vilette, D.; Guiraud, P.; Arlotto, M.; Riondel, J.; Laude, H.; Lehmann, S.; Favier, A. *J. Biol. Chem.* **2003**, *278*, 9064.
44. Rachidi, W.; Mange, A.; Senator, A.; Guiraud, P.; Riondel, J.; Benboubetra, M.; Favier, A.; Lehmann, S. *J. Biol. Chem.* **2003**, *278*, 14595.
45. Li, Q. X.; Luo, Q. H.; Li, Y. Z.; Shen, M. C. *Dalton Trans.* **2004**, 2329.
46. Totte, J.; Scharpe, S.; Verkerk, R.; Neels, H.; Vanhaeverbeek, M.; Smitz, S.; Rousseau, J. J. *Lancet* **1981**, *1*, 1047.

FULL PAPER *Clinical Pathology*

Sequence Variation of Bovine Prion Protein Gene in Japanese Cattle (Holstein and Japanese Black)

Satoshi NAKAMITSU[1)], Takayuki MIYAZAWA[1)], Motohiro HORIUCHI[2)], Sadao ONOE[3)], Yasunori OHOBA[4)], Hitoshi KITAGAWA[4)] and Naotaka ISHIGURO[5)]*

[1)]*Laboratory of Veterinary Public Health, Obihiro University of Agriculture and Veterinary Medicine, Obihiro, Hokkaido 080–8555,* [2)]*Laboratory of Prion Disease, Graduate School of Veterinary Medicine, Hokkaido University, Sapporo, Hokkaido 060–0813,* [3)]*Molecular Biotechnology Laboratory, Hokkaido Animal Research Center, Shintoku, Hokkaido 081–0038,* [4)]*Laboratories of Internal Medicine and* [5)]*Food and Environmental Hygiene, Faculty of Applied Biological Science, Gifu University, Gifu 501–1193, Japan*

(Received 9 June 2005/Accepted 16 September 2005)

ABSTRACT. To assess relationships between nucleotide polymorphisms of the prion protein (*PRNP*) gene and susceptibility to bovine spongiform encephalopathy (BSE), we investigated polymorphisms in the open reading frame (ORF) and 2 upper regions of the *PRNP* gene from 2 Japanese cattle breeds: 863 healthy Holstein cattle, 6 BSE-affected Holstein cattle, and 186 healthy Japanese Black (JB) cattle. In the ORF, we found single-nucleotide polymorphisms (SNPs) at nucleotide positions 234 and 576 and found 5 or 6 copies of the octapeptide repeat, but we did not find any amino acid substitutions. In the upper region, we examined 2 sites of insertion/deletion (indel) polymorphisms: a 23-bp indel in the upper region of exon 1, and a 12-bp indel in the putative promoter region of intron 1. A previous report suggests that the 23-bp indel polymorphism is associated with susceptibility to BSE, but we did not find a difference in allele frequency between healthy and BSE-affected Holstein cattle. There were differences in allele frequency between healthy Holstein and JB cattle at the 23- and 12-bp indels and at the SNPs at nucleotide positions 234 and 576, but there was no difference in allele frequency of the octapeptide repeat. We identified a unique *PRNP* gene lacking a 288-bp segment (96 amino acids) in DNA samples stocked in our laboratory, but this deletion was not found in any of the 1049 cattle examined in the present study. The present results provide data about variations and distribution of the bovine *PRNP* gene.

KEY WORDS: BSE, cattle, polymorphism, prion, *PRNP*.

J. Vet. Med. Sci. 68(1): 27–33, 2006

Transmissible spongiform encephalopathies (TSEs) are a group of fatal neurodegenerative diseases that include Creutzfeldt-Jakob disease (CJD), Gerstmann-Sträussler-Scheinker syndrome (GSS), Kuru and fatal familial insomnia (FFI) in humans, scrapie in sheep and goats, chronic wasting disease (CWD) in deer and elk, feline spongiform encephalopathy (FSE) in cats, transmissible mink encephalopathy (TME) in minks, and bovine spongiform encephalopathy (BSE) in cattle [26,27]. The hallmarks of TSE are neuronal vacuolation, astrocytosis, and accumulation of a pathogenic, abnormal and protease-resistant isoform of prion protein (PrP), designated PrP^{Sc} or prion, in the central nervous system. PrP^{Sc} is generated from the endogenous cellular prion protein PrP^{C}, encoded by the prion protein gene (*PRNP*), by post-translational modification leading to conformational changes [26, 27]. It has been hypothesized that PrP^{C} plays a role in copper metabolism [20, 32], but the normal functions of PrP^{C} in cells are unclear.

It is generally believed that BSE epidemics in cattle are caused by ingestion of meat and bone meal contaminated with PrP^{Sc} [35]. BSE appears to pose a threat not only to cattle but also to human public health, because the human disease variant CJD (vCJD) is thought to be caused by ingestion of meat or meat products contaminated with BSE [3, 30]. Genetic resistance to TSE is thought to be an important factor in prevention of disease recurrence. In the open reading frame (ORF) of the *PRNP* gene, amino acid polymorphisms associated with prion disease susceptibility and incubation period have been found in humans [24], sheep [2, 4, 13] and mice [34]. Sheep with valine at codon 136 and glutamine at codon 171 ($V^{136}Q^{171}$ animals) exhibit high susceptibility and short incubation period for scrapie, whereas sheep with alanine at codon 136 and arginine at codon 171 ($A^{136}R^{171}$ animals) exhibit resistance to scrapie [2, 13]. An analysis of the ORF of the *PRNP* gene of cattle (*Bos Taurus*) revealed several nucleotide substitutions including an octapeptide repeat polymorphism, but it is unclear whether the polymorphisms correlate with BSE [6, 12,14, 23, 28].

In Japan, the first BSE-affected animal was found in September 2001, and a total of 20 BSE-infected cattle have been found at end of July, 2005. There have been few reports about sequence variations in the *PRNP* gene of Holstein and Japanese Black (JB) cattle, which are widely raised in Japan [31]. The purpose of the present study was to examine variations of the *PRNP* gene in Holstein and JB cattle in Japan, including estimation of the relationship between bovine *PRNP* polymorphisms and occurrence of BSE.

MATERIALS AND METHODS

Animals and DNA samples: We examined 1049 healthy cattle: 863 Holstein cattle from Hokkaido Prefecture in Japan (489 cattle from 8 dairy farms, and 374 cattle from a

* CORRESPONDENCE TO: ISHIGURO, N., Laboratory of Food and Environmental Hygiene, Faculty of Applied Biological Science, Gifu University, Gifu, 501–1193, Japan.

slaughterhouse), and 189 JB cattle from 5 districts in Gifu Prefecture. We also examined 6 BSE-affected Holstein cattle, from Hokkaido (3 cases), Gunma (1 case), Kanagawa (1 case) and Wakayama (1 case) Prefectures (http://www.mhlw.go.jp/topics/0103/tp0308-1.html). DNA was isolated from blood samples from healthy Holstein and JB cattle, and from meat or the medulla oblongata of BSE-affected cattle, using the QIAamp DNA Blood Mini Kit (Qiagen Science, Germantown, MD). Blood was also directly used for polymerase chain reaction (PCR) with an Ampdirect kit (Shimadzu biotech, Kyoto, Japan). The 52 DNA samples (15 samples from sporadic bovine leucosis, 6 samples from enzootic bovine leucosis, 5 samples from tumor, 16 samples from the other diseases and 10 samples from healthy cattle) stocked in our laboratory were examined in the present study.

DNA amplification: We examined 3 regions for nucleotide polymorphisms: a 23-bp indel polymorphism about 1.5 kb upstream of exon 1, a 12-bp indel polymorphism in intron 1, and the entire ORF of exon 3. To determine DNA sequences, 795 bp of the ORF of the bovine *PRNP* gene (nt 65579 to 66373 in accession number AJ298878 [9]) were amplified using the primers BPrP3 (5'GCAGATATAAGTCATCATGGTG) and BPrP4 (5'GAAGATAATGAAAACAGGAAGG), as described by Gombojav *et al.* [7] (Fig. 1). To assay the octapeptide (PHGGGWGQ) repeat and the 288-bp deletion in the ORF of the bovine *PRNP* gene, we directly amplified the N-terminal region (577 to 565 bp) of the ORF using 0.7 μl of blood (863 Holstein and 186 JB cattle) in 25 μl of Ampdirect buffer containing 1 unit of Taq polymerase (Sigma Aldrich, St. Louis, MO), 10 pmol of the primers BPrP3 and SP4 (5'CATTGGTCTTGTTGAAACAC) and 2 mM dNTPs, according to the Ampdirect kit instructions. To examine the 23-bp insertion/deletion (indel) polymorphism in the upper region of exon 1 (A, 23-bp indel in Fig. 1), we amplified 123 or 100 bp using the primers PRNP47784 and PRNP47883R and DNA specimens from 278 Holstein and 186 JB cattle [28]. For the 12-bp indel polymorphism in intron 1 of the bovine *PRNP* gene (B, 12-bp indel in Fig. 1), we amplified 414 or 426 bp using the primers BPrP30 (5'CTTCTCTCTCGCAGAAGCAG) and BPrP32 (5'CCCTTGTTCTTCTGAGCTCC) and DNA specimens from 290 Holstein and 186 JB cattle. The thermal cycling sequence of the amplification was as follows: initial denaturation at 94°C for 10 min; 50 cycles of denaturation at 94°C for 30 s, annealing at the annealing temperature of the specific primer pair for 30 s, and extension at 72°C for 1 min; final extension at 72°C for 7 min. All PCR products were electrophoresed to assess yield and purity on 1.5% to 3.0% agarose gels, and were then photographed. The PCR product for the 12-bp indel (414 or 426 bp) was digested with *Sac*II enzyme and separated on 2% agarose gel to assay for the presence of the 12-bp indel, because the 12-bp indel sequence contains a *Sac*II recognition site.

DNA sequencing: PCR products were purified using the QIAquick PCR Purification Kit (Qiagen) for DNA sequencing. Purified PCR products of the bovine *PRNP* gene were directly sequenced using internal sequencing primers SP1 (5'TTGGTGGCTACATGCTGGGAAG) and SP4. Sequencing was performed using an ABI 310 DNA sequencer with an ABI PRISM BigDye Terminator v3.1 Cycle Sequencing Kit. Alignment of sequences was performed using GENETYX-MAC software (Software Development Co., Tokyo, Japan).

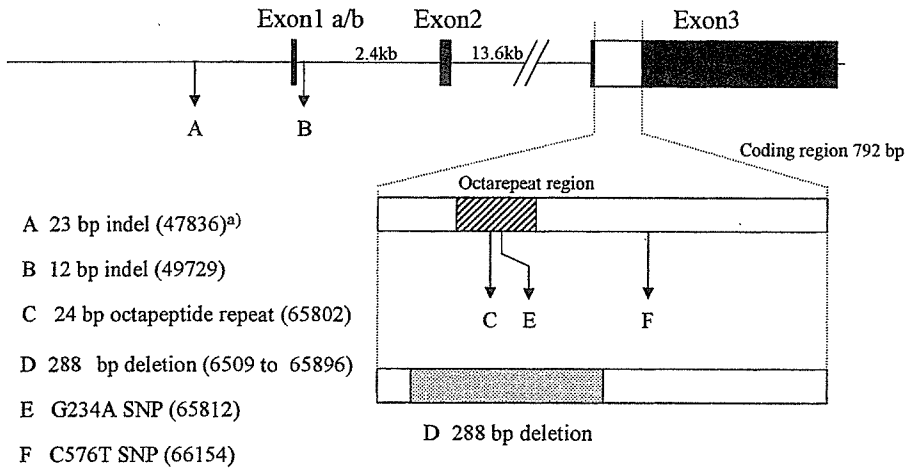

Fig. 1. Diagram of genomic structure of the bovine *PRNP* gene. The 6 polymorphisms (3 indels, 1 deletion and 2 SNPs) found in the present study are indicated by arrows labeled with letters. The 3 *PRNP* exons are represented by black boxes, and the protein-coding region in exon 3 is shown as a white area in the black box [11]. The hatched portion of the coding region indicates the octarepeat region. The dotted portion of the coding region indicates the 96-amino-acid (288-bp) deletion from nt 65609 to 65896 in reference sequence AJ298878 [9]. a) The numbers in parentheses indicate positions in reference sequence AJ298878.

Statistical analysis: We used the χ-square test to assess the significance of associations between allele distribution and BSE among Holstein and JB cattle.

RESULTS

Polymorphisms in the upstream region: Representative results for the 23-bp indel are shown in Fig. 2A. Cattle homozygous for the 23-bp deletion or insertion showed one distinct band, at 100 or 123 bp, respectively (Fig. 2A, designated by –/– and +/+). Cattle heterozygous for the 23-bp indel showed two bands: at 123 and 100 bp (Fig. 2A, +/–). The majority of the Holstein cattle tested for the 23-bp indel (62%) were homozygous for the 23-bp deletion, whereas the majority of the JB cattle (61%) were heterozygous for the 23-bp indel (Table 1). For cattle homozygous for the 12-bp insertion, the *Sac*II enzyme cleaved the PCR product (426 bp) into two fragments: 276 and 150 bp. Cattle homozygous for the 12-bp deletion showed a single band at 414 bp. Cattle heterozygous for the 12-bp indel showed three distinct bands: 414, 276 and 150 bp (Fig. 2B, +/–). Most of the Holstein cattle tested for the 12-bp indel were either heterozygous or were homozygous for the 12-bp deletion, but 61% of the JB cattle were heterozygous.

Among the 6 BSE-affected cattle, 2 cattle were heterozygous at both the 23- and 12-bp indels, and 4 cattle were homozygous at both the 23- and 12-bp indels.

Polymorphisms of ORF in PRNP: In the present study, we found a mutant with a 288-bp deletion (96 amino acids from codon 11 to codon 108) among 52 DNA samples stocked in our laboratory (Fig. 1). The N-terminal region amplified from the 288-bp-deletion mutant showed two bands: one band containing 6 copies of the octapeptide repeat (575 bp), and the other small band (287 bp) with the 288-bp deletion (Fig 2D). None of the 1049 cattle tested carried the 288-bp deletion in the *PRNP* gene. Among both Holstein and JB cattle, the predomininat genotype of the octapeptide repeat was homozygosity for the 6-copy allele (575 bp in Fig. 2C, designated as 6/6), followed by heterozygosity for 5 and 6 copies (Fig. 2C, 6/5) (Table 1). Only 4 Holstein cattle and none of the JB cattle were homozygous for 5 copies of the octapeptide repeat (Fig. 2C, 5/5). All BSE-affected cattle had 6 copies of the octapeptide repeat. We detected 2 single-nucleotide polymorphisms (SNPs) at G234A and C576T in 232 Holstein and 186 JB cattle (Table 1). At the C576T SNP, none of the Holstein cattle were homozygous for thymine, but 28 of the JB cattle were homozygous for thymine.

Statistical analysis of nucleotide polymorphisms: Allele frequencies of nucleotide polymorphisms at the 2 indels (23 and 12 bp), the octapeptide repeat and 2 SNPs (nt 234 and 576) are shown in Table 2. There was no significant difference between healthy and BSE-affected Holstein cattle at any of the nucleotide polymorphisms. At the 23- and 12-bp indels and the G234A and C576T SNPs, there were significant differences in allele frequency between healthy Holstein and JB cattle (Table 2).

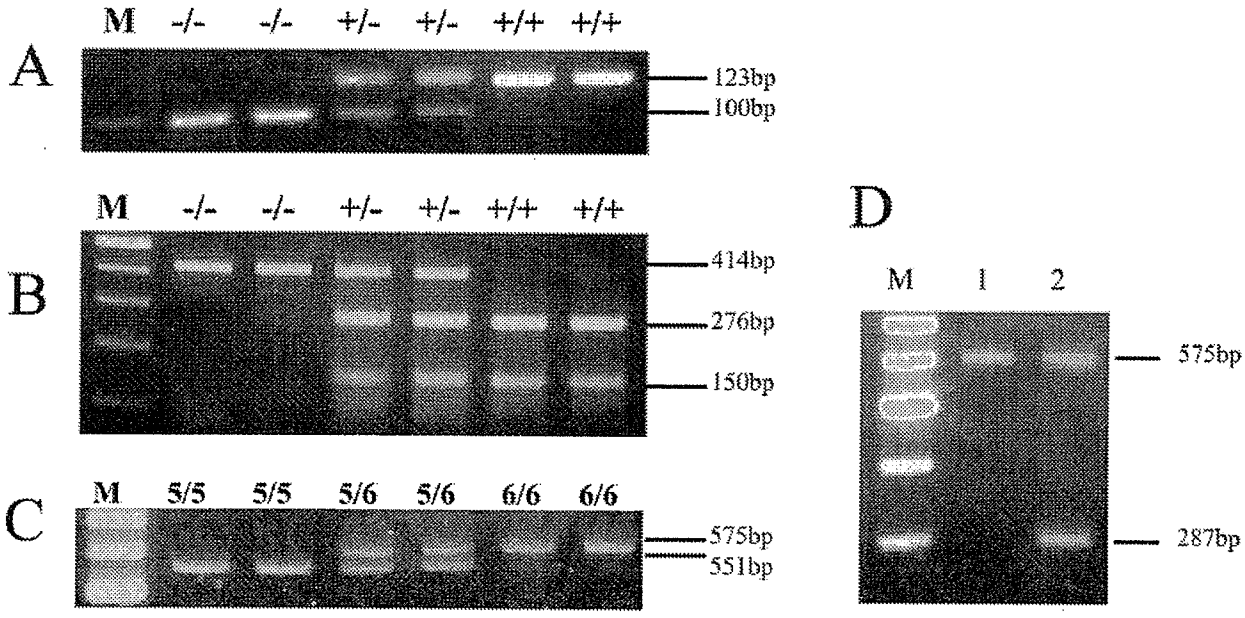

Fig. 2. Genotyping of insertion or deletion polymorphisms by agarose gel electrophoresis. A) Genotypes of 6 different cattle are indicated as presence (+) or absence (–) of 23-bp insertion. B) Genotypes of *Sac*II-digested PCR products from 6 different cattle are indicated as presence (+) or absence (–) of 12-bp insertion. C) Genotypes of octapeptide repeats (homozygote 5/5, heterozygote 5/6 and homozygote 6/6). D) Genotypes of N-terminal region of *PRNP* gene amplified using primers BPrP3 and SP4: lane 1, PCR product from 6/6 homozygote; lane 2, PCR product from 288-bp-deletion mutant. M, 100-bp DNA size marker.

Table 1. Genotype frequency of polymorphisms among healthy Holstein, healthy JB cattle and BSE-affected Holstein cattle

Breed and location		N[f]	23-bp indel[a]			12-bp indel[b]			Octarepeat[c]			G234A[d]			C576T[e]		
			+/+	+/–	–/–	+/+	+/–	–/–	6/6	6/5	5/5	G/G	G/A	A/A	C/C	C/T	T/T
Healthy Holstein	A	15	1	8	6	2	8	5	13	2	0	6	7	2	15	0	0
	B	27	3	12	11	4	16	6	23	4	0	17	7	3	27	0	0
	C	168	0	36	127	0	45	117	148	19	1	59	11	4	72	2	0
	D	74	10	34	30	11	37	26	61	13	0	–	–	–	–	–	–
	E	13	–	–	–	4	4	5	10	3	0	7	2	4	13	0	0
	F	51	–	–	–	–	–	–	47	4	0	32	10	9	51	0	0
	G	125	–	–	–	–	–	–	109	14	2	43	9	0	52	0	0
	H	16	–	–	–	–	–	–	14	2	0	–	–	–	–	–	–
	I	374	–	–	–	–	–	–	340	33	1	–	–	–	–	–	–
Total healthy Holstein		863	14	90	174	21	110	159	765	94	4	164	46	22	230	2	0
Healthy JB[g]																	
	J	37	3	29	5	3	26	8	37	0	0	6	25	6	13	20	4
	K	37	7	24	6	10	22	5	30	7	0	11	19	7	18	14	5
	L	31	0	11	20	0	13	18	28	3	0	16	15	0	4	16	11
	M	40	4	22	14	6	24	10	37	3	0	13	21	6	17	20	3
	N	41	5	28	8	5	28	8	41	0	0	10	27	4	15	21	5
Total healthy JB		186	19	114	53	24	113	49	173	13	0	56	107	23	67	91	28
Total healthy Holstein and healthy JB		1049	33	204	227	45	223	208	938	107	4	220	153	45	297	93	28
BSE-affected Holstein		6	0	2	4	0	2	4	6	0	0	4	1	1	6	0	0

a) The 23-bp indel polymorphism in the upper region of exon 1 in Fig.1.
b) The 12-bp indel polymorphism in intron 1 in Fig.1.
c) Octarepeat polymorphism of the coding region.
d),e) Polymorphism at nt 234 and 576 in the ORF, respectively.
f) Number of samples collected.
g) JB, Japanese Black.

Table 2. Allele frequency of nucleotide polymorphisms among healthy Holstein, healthy JB cattle and BSE-affected Holstein cattle

Breed	Nucleotide polymorphisms																	
	23-bp insertion				12-bp insertion				Octarepeat[c]				G234A				C576T			
	n[a]	+[b]	–[c]	p[d]	n	+	–	p	n	6	5	p	n	G	A	p	n	C	T	p
Healthy Holstein	278	0.21	0.79		290	0.26	0.74		863	0.94	0.06		232	0.81	0.19		232	1.00	0	
BSE Holstein	6	0.17	0.83	n.s[f]	6	0.17	0.83	n.s	6	1.00	0	n.s	6	0.75	0.25	n.s	6	1.00	0	n.s
Subtotal	284	0.21	0.79		296	0.27	0.74		869	0.94	0.06		238	0.80	0.20		238	1.00	0	
Healthy JB	186	0.41	0.59	<0.01	186	0.43	0.57	<0.01	186	0.97	0.03	n.s	186	0.56	0.41	<0.01	186	0.60	0.40	<0.01
Healthy JB and Holstein	464	0.29	0.71		476	0.33	0.67		1049	0.95	0.05		418	0.71	0.29		418	0.82	0.18	

a) n, number of cattle examined.
b) +, 23-bp or 12-bp insertion.
c) –, 23-bp or 12-bp deletion.
d) $p<0.01$, significant difference among the compared values.
e) Five or 6 copies of octapeptide repeat.
f) n.s, not significant.